Communications
doi.org/10.1002/batt.201900226

Chemistry Europe
European Chemical Societies Publishing

Special Collection

Electric Double-Layer Capacitors Based on Non-Aqueous Electrolytes: A Comparative Study of Potassium and Quaternary Ammonium Salts

Satoshi Uchida*[a] and Titus Masese*[a]

Immense attention has been drawn towards electric double layer capacitors (EDLCs) as a viable intermittent energy storage solution, owing to their ultra-fast charge/discharge rates and long cycle life. However, the high activation energy of ionic conductivity innate in conventional aprotic organic electrolytes has greatly impeded the feasibility of high-performance EDLCs. Herein, we investigate and compare the physicochemical properties and performance of electrolytes based on potassium hexafluorophosphate (KPF_6) and commercial triethylmethylammonium tetra-fluoroborate ($TEMABF_4$) salts in EDLCs. Compared to commercial $TEMABF_4$-based electrolytes, KPF_6 salt-based electrolytes (in acetonitrile solvent) demonstrate outstanding rate performance. The KPF_6 salt-based electrolyte further manifests lower ionic resistance within activated carbon pores as well as lower interfacial resistance between electrode and electrolyte; an affirmation of not the high ionic conductivity but rather the eminence of low activation energy. The low activation energy can be attributed to the low effective nuclear charge of the K^+ cations that allow anions to transverse easily in solvent state. This study not only underpins potassium-ion (K^+) as a fast charge carrier, but also a viable solution for the next-generation non-aqueous power devices relying on monovalent alkali cations.

As the pursuit of energy security and environmental sustainability heightens, a strong demand for large-scale and capacious energy storage systems has quickly emerged. Rechargeable battery technology such as lithium-ion batteries has dominated the energy sector due to their high energy densities. However, their slow charge/discharge rates and poor cycle life render them unsuitable for applications such as regenerative power systems. As a result, energy and material scientists have shifted focus into electric double layer capacitors (EDLCs), for their ultra-fast charge/discharge rates and long cycle life.

[a] *Dr. S. Uchida, Dr. T. Masese*
Department of Energy and Environment
Research Institute of Electrochemical Energy
National Institute of Advanced Industrial Science and Technology
1-8-31 Midorigaoka, 563-8577, Ikeda, Japan
E-mail: satoshi-uchida@aist.go.jp
titus.masese@aist.go.jp

Supporting information for this article is available on the WWW under https://doi.org/10.1002/batt.201900226

Special Collection *An invited contribution to a Special Collection on Electrolytes for Electrochemical Energy Storage*

Unlike batteries that rely on slow chemical reactions for charge storage and discharge, EDLCs charge/discharge mechanism is ultra-fast adsorption/desorption of ions at the interface between the electrodes and the electrolyte, endowing them with remarkable rate capabilities and long cycle life.[1–3] These attributes make ELDCs favorable for high power operations. In high-voltage operations, aprotic organic electrolytes based on propylene carbonate (PC) or acetonitrile (AN) solvents are generally preferred due to their higher voltage tolerance (wider potential window) compared to aqueous electrolytes.[4,5] Thus, typical commercial high-performance EDLCs incorporate electrolytes that consist of solvents dissolved in quaternary ammonium cations (namely, R_4N^+).[6,7] The large ionic radii of R_4N^+ only allows few anions, with small stokes radii to bind or interact with it in the electrolyte; endowing it with high ionic conduction essential to the operation of the EDLCs.

In principle, the capacitance of an electric double-layer is inversely proportional to its thickness; a parameter that is highly dependent on the ionic radii.[1] Therefore, for rapid charge and discharge, high ionic conduction is fundamental; making the use of small stokes radii ions more desirable for the EDLC electrolytes. In this regard, lithium-ions (Li^+) may seem as suitable cations for non-aqueous EDLCs due to their desirably small ionic radii. However, their extremely high charge-density causes strong interactions with solvents and behaves as solvated-Li^+, radii of which is larger than that of solvated-R_4N^+.[8] In fact, if a lithium salt or a R_4N salt consisting of different anions are dissolved in the same solvent, the latter shows higher molar conductivity and higher cation-limited molar conductivity.[9] Hence, the use of Li^+ would be inexpedient for both the rate performance and capacitance of EDLCs.[10,11]

As such, monovalent alkali cations with stokes radius comparable to R_4N, would be applicable. Potassium-ion (K^+) are known to have relatively smaller stokes radii in aqueous solution, which make them possible to facilitate faster conduction than Li^+.[12,13] In this context, the application of K^+ as charge carriers in organic electrolytes could also be hypothesized.[14] Thus, electrical energy storage devices that utilize K^+ as the charge carrier can be expected to show good rate performance. In this study, we report the physicochemical of electrolytes containing K^+ or R_4N^+ and compare their performance when used in EDLC.

In this study, electrolytes comprising triethylmethylammonium tetrafluoroborate ($TEMABF_4$) salt, which is commonly used in commercial EDLCs, and potassium hexafluorophosphate (KPF_6) salt were selected for a comparative study.

For a more explicit comparison with commercially-used $TEMABF_4$, potassium tetrafluoroborate (KBF_4) salt would serve as a better electrolyte for potassium-based EDLC to clearly elaborate properties such as the cationic behavior. However, KBF_4 hardly dissolves in the various organic solvents selected over the course of this study and attempts to obtain high-purity $TEMAPF_6$ were elusive - the only highly pure salt available was $TEMABF_4$ which also presents higher ionic conductivity amongst other quaternary ammonium salts based on tetrafluoroborates.[6,15,16] As a solution, KPF_6 was selected for this study. KPF_6 was dissolved in acetonitrile (AN) solvent to prepare an electrolyte solution conforming to common concentrations of 0.8 mol dm^{-3} (which is close to saturation at 25 °C) and $TEMABF_4$ was dissolved in acetonitrile (AN) solvent to prepare an electrolyte solution with concentrations of 1.5 and 0.8 mol dm^{-3}. For brevity, these electrolytes are hereafter labeled as 0.8 M-KPF_6, 1.5 M-$TEMABF_4$ and 0.8 M-$TEMABF_4$. It is also important to note here that a 1.5 M-$TEMABF_4$ was also chosen as the electrolyte as it presents the highest ionic conductivity (Table S1).

Figure 1 shows a comparison of the charge-discharge curves at various current densities, namely, 2.5 mA cm^{-2} (a) and 100 mA cm^{-2} (b), and the corresponding rate performance (c) of the EDLC cells assembled using the aforementioned three electrolytes. The capacitance is calculated based on the following equation [Eq. (1)]:

$$C = \frac{I\,t}{V_{/2}\,m} \tag{1}$$

where C is the capacitance of a single electrode, I is the discharge current, t is the time, V is the operating voltage and m is the mass of the activated carbon on an electrode. At a current density commensurate to 2.5 mA cm^{-2}, almost linear and line-symmetric shape of the curve were observed, indicating that the charge and discharge process ideally progress only via the electric double-layer (EDL). Moreover, all the cells show excellent capacitance retention after 1000 times of cycle test (shown in Figure S1), which implies that side reactions hardly occur. The capacitance of EDL significantly relates to the pore diameter and the ionic radii,[17–19] of which, if matched leads to a profound increase in the capacitance.[19] Hence, it is considered that the reason why the capacitance of KPF_6 system is slightly lower than those of $TEMABF_4$ is that the pore diameter of the activated carbon, used in the present study, is optimized for the latter. The voltage (also referred to as "ohmic" or denoted as 'IR') drop at the beginning of discharging curve derived from the internal resistance of the cells, which is too small to be observed at 2.5 mA cm^{-2}, becomes pronounced significantly with increasing current densities. At a current drain of 100 mA cm^{-2}, the 0.8 M-KPF_6 system shows smaller IR drop as compared to those with 0.8 M- and 1.5 M-$TEMABF_4$ ones, which leads to superior rate performance among them.

To further investigate the factors underlying the superior rate performance of potassium-based EDLCs, impedance measurements were duly performed, details of which are furnished in the Experimental section. Figure 2 displays the Nyquist plots obtained from the alternating current (AC) impedance measurement of the cells after rate performance test, where the total impedance can be divided into various resistance components.[20] To simplify the discussion, the Z_{Re}-axis intercept, which corresponds to the resistance of bulk electrolyte solution (R_s) in the separator of which the thickness is not necessarily the same in all cells, has been set to 0 Ω in Figure 2. Note that the magnitude relationship of the total impedance among the three cells is not changed by the offset. Uncorrected data is furnished in Figure S2. The semicircular feature emanates from the electrical contact resistance in the activated carbon electrode[21,22] (R_e) and the interfacial impedance between the electrode and the electrolyte[23,24] (R_{int}).

As the cells were assembled with same electrode, the difference in the magnitude of the semi-circle seems to be dominated by electrolyte, that is, 0.8 M-KPF_6 shows lower R_{int} as compared to 0.8 M- and 1.5 M-$TEMABF_4$. The straight line with a 45° slope reflects the ion diffusion impedance in the pore of activated carbon[25] (R_{ion}). Although K^+, with a relatively high charge-density, should be solvated by several solvent molecules to migrate, velocity of which is not as fast as un-solvated ions, 0.8 M-KPF_6, unpredictably, shows small R_{ion} compared to both $TEMABF_4$ electrolytes. The EDL behavior appears as a

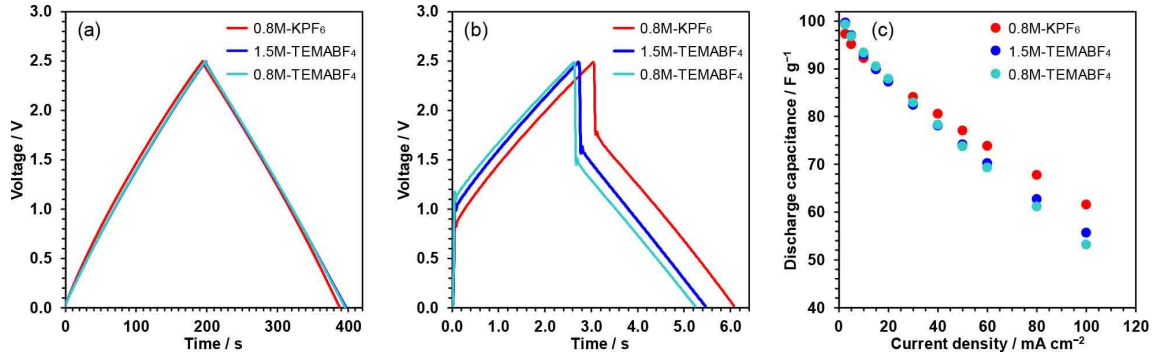

Figure 1. Charge-discharge curves at a current density corresponding to (a) 2.5 mA cm^{-2} and (b) 100 mA cm^{-2} and (c) the rate performance of the EDLC cells assembled with the three electrolytes measured after 1000 times of cycle test which also serves as pre-cycles. The measurement voltage range and temperature are, respectively, 0–2.5 V and 25 °C. Ten cycles were performed at each current density of which data for respective 6th cycle is used in this figure. For clarity, note that all the EDLC components used in this comparative study are the same, apart from the electrolyte.

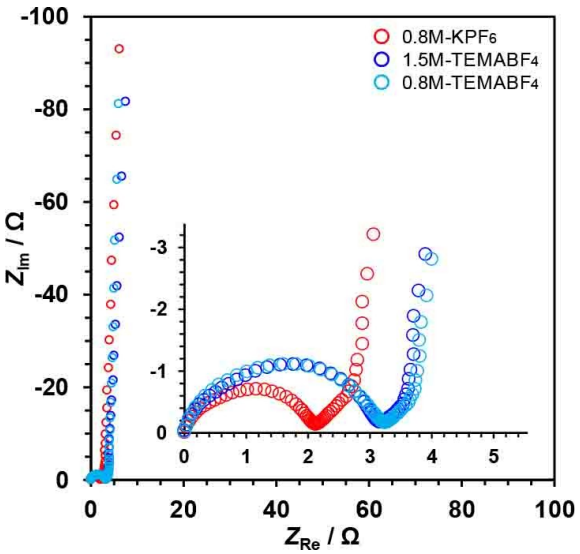

Figure 2. Compensated Nyquist plot obtained from AC impedance measurement after rate performance test of the cells assembled with the three electrolytes. The frequency range, AC amplitude and measurement temperature are 1 MHz–10 MHz, 5 mV and 25 °C, respectively. The inset shows an enlarged figure of the high- to medium-frequency regions.

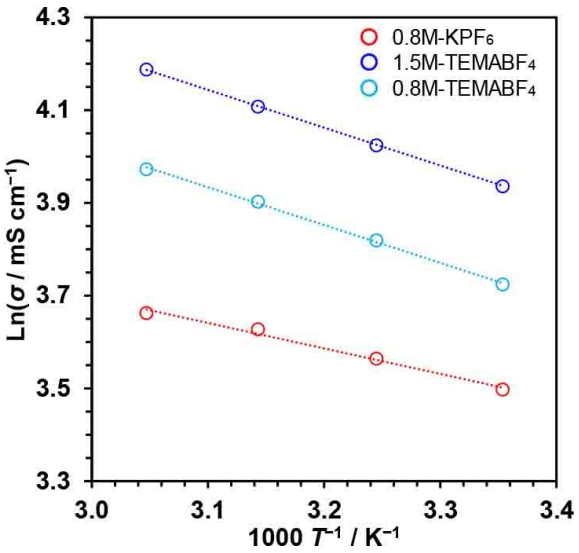

Figure 3. Logarithmic plots of the specific conductivity (ln σ) of the three electrolyte solutions against the reciprocal of temperature (1/T), of which the slope gives $-E_a/R$ value, measured by AC impedance spectroscopy in a four-electrode cell. Numerical data are available in Table S1.

subsequent vertical line which gives the differential capacitance (denoted as C_{diff}) calculated by the following equation [Eq. (2)]:[26,27]

$$C_{diff} = \frac{1}{2\pi f Z_{Im}} \quad (2)$$

where f and Z_{Im} denote the frequency and imaginary part of arbitrary plot on the vertical line respectively. The C_{diff} value for the various electrolytes when used in the EDLC is in the following sequence: 0.8 M-KPF_6 < 1.5 M-$TEMABF_4$ = 0.8 M-$TEMABF_4$. This trend is the same as the capacitance observed in the cycle test (see Figure 1S), due to the aforementioned reason.

Figure 3 shows the Arrhenius plots of the ionic conductivity (σ) of 0.8 M-KPF_6, 0.8 M-$TEMABF_4$ and 1.5 M-$TEMABF_4$. The numerical data are displayed in Table 1S, which also provides the activation energy (E_a) derived from Arrhenius equation [Eq. (3)]:[28,29]

$$\sigma = A \exp\left(-\frac{E_a}{RT}\right) \quad (3)$$

where the symbols A, R and T represent the frequency factor, the gas constant and the absolute temperature, respectively. The three electrolyte solutions manifest completely different ionic conductivities, which do not seem to correspond to the R_{ion} and the R_{int}. A case that would serve as a clear example that the ionic behavior at the interface and in the pores is not dominated by the bulk properties.

On the other hand, R_{ion} and R_{int} are strongly influenced by the E_a, which is also derived from the bulk conductivity. It is however reasonable to infer that the E_a has a certain correlation with the ionic behavior even in the micro-space, since it is the minimum energy that must be added to move ions. 0.8 M- and 1.5 M-$TEMABF_4$ show essentially the same E_a, which means that the environment surrounding $TEMA^+$ and BF_4^- in them are exactly the same as each other. As a matter of fact, 0.8 M-KPF_6 shows a different activation energy whose lower value is thought to be attributed to the K^+ mobility, as the limiting molar conductivity of PF_6^- is reported to be smaller than that of BF_4^-.[4]

Figure 4 compares the Raman spectra of 0.8 M-KPF_6, 0.8 M-$TEMABF_4$ and 1.5 M-$TEMABF_4$. The peaks centered around 2254 cm^{-1} are assigned to stretching vibration of C≡N bonds in free AN molecules.[30,31] No peak shift is observed in the $TEMABF_4$ electrolytes, which indicates that AN does not solvate

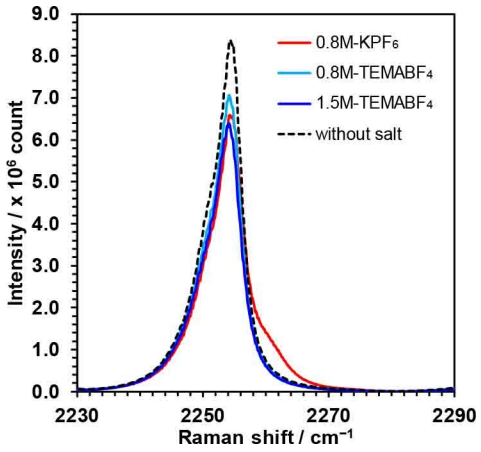

Figure 4. Raman spectra at room temperature for acetonitrile (AN) solvent and electrolytes consisting of 0.8 M-KPF_6, 0.8 M-$TEMABF_4$ and 1.5 M-$TEMABF_4$ dissolved in AN. The peak of which the top is located at 2254 cm^{-1} arises from the stretching modes of C≡N bonds in AN molecular.

at all. The shoulder observed around 2262 cm^{-1} in 0.8 M-KPF_6 indicates the solvation of several AN to K^+, which hardly occurs on anions (see also Figure S3). The solvation of AN to K^+ is in line with the recent reports by Amara and co-workers.[32] Compared with the spectrum of 0.8 M-$LiPF_6$ (shown in Figure S4), remarkably small peak shifts of 0.8 M-KPF_6 implies that the interaction between K^+ and AN is quite weak, that is, K^+ probably can be released from some AN dynamically in presence of an electric field, thus exhibiting the low activation energy (E_a).

The present study also compared the behavior of K^+ and $TEMA^+$ electrolytes in micro-space (such as the pore and the interface). Results indicated that in micro-space, K^+ electrolyte is dominated by the activation energy (E_a) rather than by ionic conductivity. The low E_a of 0.8 M-KPF_6, enables it to achieve excellent rate performance in EDLC operations.

These results prove that K-ions (K^+) can be excellent charge carriers not only in aqueous electrolytes but also in organic ones, a factor attributed to the weak interaction between K^+ and the solvent; owing to its relatively low charge-density compared with Li^+ *etc.*, and solvent molecules. Compared to the behavior of Li^+ in non-aqueous electrolytes, not many reports on K^+ in non-aqueous electrolytes have been made. Even so, the study on K-ion batteries as alternative energy storage devices to Li-ion ones has been ongoing in recent years.[33–35] The results of this study opens up a myriad of possibilities fundamental for further exploration of potassium salt based non-aqueous electrolyte in the pursuit of comparatively cost-effective, relatively high performance electrolytic solutions hereafter.

Experimental Section

Super Dehydrated acetonitrile (AN) (Kishida Chemicals, 99% purity (battery grade)), KPF_6 (Alfa Aesar, 99% purity) and $TEMABF_4$ (Tokyo Kasei, purity of >98%) were used as-purchased. The electrolyte solutions were prepared in an argon-filled glove box with a dew point of below −70 °C to avert any side reactions with moisture. Electrolyte based on $LiPF_6$ (Kishida chemical, lithium battery grade) was also prepared to compare their ionic conduction behavior and the solvation state of cations.

The ionic conductivity of the electrolytes was measured using a potentiogalvanostat (Ivium, CompactStat.e) equipped with a frequency response analyzer and a four-electrode cell (EC frontier) which was assembled with 10 ml of each electrolyte and hermetically sealed in the glove box. The cell constant was calibrated using KCl as a conductivity standard solution. Alternating current (AC) impedance was measured at 25 °C, 35 °C, 45 °C and 55 °C within an accuracy of ±0.1 °C. The AC frequency range was set from 100 kHz to 100 Hz with an amplitude of 5 mV. Values for ionic conductivity were calculated based on the average of the real component of the obtained complex impedance data and the cell constant. Note that the measurements were performed several times, as is customary, and only reproducible results were obtained.

Activated carbon (Kuraray, YP50F), acetylene black (Denka, Li-400), sodium carboxymethyl cellulose (DKS, WSA), and styrene-butadiene rubber (JSR, TRD2001) were homogeneously dispersed in deionized water with a weight ratio of 90:5:3:2 and the obtained slurry was cast on an etched Al-foil current collector (JCC, 20CB). After drying under vacuum and pressing, the electrode sheet was cut into 12-mm diameter disks for the electrochemical measurements. The mass loading of active material was about 4.0 mg cm^{-2}. The EDLC, which is composed of two pieces of the activated carbon electrode, a glass fiber filter as the separator (Advantec, GA-100, 0.44 mm thickness) and the aforementioned electrolytes, was assembled in an argon-filled globe box by using CR2032-type coin cells (Hohsen Corp.).

The assembled EDLCs were cycled 1000 times by galvanostatic charge-discharge with a current density equivalent to 2.5 mA cm^{-2} in the voltage range of 0–2.5 V to evaluate their cycle stability, which also serves as pre-cycles. This was followed by the rate performance tests from 2.5 to 100 mA cm^{-2} in the same voltage range, where ten cycles were performed at each current value of which, data for the respective 6th cycle is used in the Figure 1. After the rate performance test, the cells were again cycled 10 times at 2.5 mA cm^{-2} and then rested at open circuit voltage for 1 h. The internal resistance of the cells was measured by the AC impedance technique. The AC frequency ranged from 500 KHz to 10 MHz with an amplitude of 5 mV. All the electrochemical measurements for the EDLC cells were carried out by using a multi electrochemical measurement system (Hokuto Denko, HZ-Pro) at 25 °C. Note that all the EDLC components used in this comparative study are the same, apart from the electrolyte.

Raman spectra of the electrolyte solutions were measured at room temperature to investigate the solvation state around the cations by using a laser Raman microscope (RENISHAW, in Via Reflex) whose excitation source was green laser (532 nm). The solutions were filled in a quartz cell with a cross-sectional area of 1×1 cm^2 in the glove box. The exposure time was 0.5 s and the scattering spectrum was integrated 60 times. The wavenumber of the Raman shift was calibrated by the spectrum of a Si wafer standard.

Acknowledgements

We acknowledge that this paper was proofread and edited through the support provided by Edfluent services.

Conflict of Interest

The authors declare no conflict of interest.

Keywords: potassium salt-based electrolyte · electric double-layer capacitors · rate performance · solvation state

[1] B. E. Conway, Electrochemical Capacitors: Scientific Fundamentals and Technology Applications, *Kluwer* **1999**.
[2] P. Sharma and T. S. Bhatti, *Energy Convers. Manage.* **2010**, *51*, 2901–2912.
[3] G. Wang, L. Zhang, J. Zhang, *Chem. Soc. Rev.* **2012**, *41*, 797–828.
[4] M. Ue, K. Ida, S. Mori, *J. Electrochem. Soc.* **1994**, *141*, 2989–2996.
[5] T. Morimoto, K. Hiratsuka, Y. Sanada, K. Kurihara, *J. Power Sources* **1996**, *60*, 239–247.
[6] M. Ue, *Electrochim. Acta* **1994**, *39*, 2083–2087.
[7] J. Sun, M. Forsyth, D. R. MacFarlane, *J. Phys. Chem. B* **1998**, *102*, 8858–8864.
[8] G. Salitra, A. Soffer, L. Eliad, Y. Cohen, D. Aurbach, *J. Electrochem. Soc.* **2000**, *147*, 2486–2493.
[9] M. Ue, *J. Electrochem. Soc.* **1994**, *141*, 3336–3342.
[10] H. Yamada, I. Moriguchi, T. Kudo, *J. Power Sources* **2008**, *175*, 651–656.

[11] J. Chmiola, C. Largeot, P. L. Taberna, P. Simon, Y. Gogotsi, *Angew. Chem. Int. Ed.* **2008**, *47*, 3392–3395; *Angew. Chem.* **2008**, *120*, 3440–3443.
[12] J. H. Jones, *J. Am. Chem. Soc.* **1945**, 855–857.
[13] L. G. Longsworth, *J. Am. Chem. Soc.* **1932**, *2741–2758*.
[14] S. Minc, L. Werblan, *Electrochim. Acta* **1962**, *7*, 257–266.
[15] C. Zhong, Y. Deng, W. Hu, J. Qiao, L. Zhang, J. Zhang, C. Zhong, Y. Deng, W. Hu, J. Qiao, L. Zhang, J. Zhang, *Chem. Soc. Rev.* **2015**, *44*, 7484–7539.
[16] M. Ue, M. Takeda, M. Takehara, S. Mori, *J. Electrochem. Soc.* **1997**, *144*, 2684–2688.
[17] C. Merlet, M. Salanne, B. Rotenberg, P. A. Madden, *Electrochim. Acta* **2013**, *101*, 262–271.
[18] C. Largeot, C. Portet, J. Chmiola, P. Taberna, Y. Gogotsi, P. Simon, *J. Am. Chem. Soc.* **2008**, *130*, 2730–2731.
[19] D. Jiang, J. Wu, *J. Phys. Chem. Lett.* **2013**, *4*, 1260–1267.
[20] X. Liu, L. Juan, L. Zhan, L. Tang, Y. Wang, W. Qiao, X. Liang, L. Ling, *J. Electroanal. Chem.* **2010**, *642*, 75–81.
[21] C. Lei, N. Amini, F. Markoulidis, P. Wilson, S. Tennison, C. Lekakou, *J. Mater. Chem. A* **2013**, *1*, 6037–6042.
[22] C. Lei, F. Markoulidis, Z. Ashitaka, C. Lekakoua, *Electrochim. Acta* **2013**, *92*, 183–187.
[23] J. Kang, J. Wen, S. Jayaram, A. Yu, X. Wang, *Electrochim. Acta* **2014**, *115*, 587–598.
[24] H. D. Yoo, J. H. Jang, J. H. Ryu, Y. Park, S. M. Oh, *J. Power Sources* **2014**, *267*, 411–420.
[25] J. H. Jang, S. M. Oh, *J. Electrochem. Soc.* **2004**, *151*, A571–A577.
[26] H. Song, Y. Jung, K. Lee, L. Dao, *Electrochim. Acta* **1999**, *44*, 3513–3519.
[27] C. Yang, C. V. Li, F. Li, K. Chan, *J. Electrochem. Soc.* **2013**, *160*, H271–H278.
[28] N. Giroud, H. Rouault, E. Chainet, J. Poignet, *ECS Trans.* **2009**, *16*, 75–88.
[29] M. Petrowsky, R. Frech, *Electrochim. Acta* **2010**, *55*, 1285–1288.
[30] D. M. Seo, O. Borodin, S. Han, P. D. Boyle, W. A. Henderson, *J. Electrochem. Soc.* **2012**, *159*, A1489–A1500.
[31] S. Han, O. Borodin, D. M. Seo, Z. Zhou, W. A. Henderson, *J. Electrochem. Soc.* **2014**, *161*, A2042–A2053.
[32] S. Amara, J. Toulc'Hoat, L. Timperman, A. Biller, H. Galiano, C. Marcel, M. Ledigabel, M. Anouti, *ChemPhysChem.* **2019**, *20*, 581–594.
[33] T. Masese, K. Yoshii, Y. Yamaguchi, T. Okumura, Z.-D. Huang, M. Kato, K. Kubota, J. Furutani, Y. Orikasa, H. Senoh, H. Sakaebe, M. Shikano, *Nat. Commun.* **2018**, *9*, 3823.
[34] H. Kim, H. Ji, J. Wang, G. Ceder, *Trends. Chem.* **2019**, *1*(7), 682–692.
[35] K. Yoshii, T. Masese, M. Kato, K. Kubota, H. Senoh, M. Shikano, *ChemElectroChem* **2019**, *6*, 1–11.

Manuscript received: December 26, 2019
Revised manuscript received: January 15, 2020
Accepted manuscript online: January 16, 2020
Version of record online: February 3, 2020